9th Latin American Congress in Heat and Mass Transfer
San Juan, Puerto Rico
October 20-22, 2002

STUDY OF LIQUID TRANSPORT DURING DRYING OF CAPILLARY POROUS SOLIDS PARTIALLY SATURATED WITH SOLVENTS

R. Gamero[1] and J. Martínez[2]

[1]Facultad de Ingeniería Química, Universidad Nacional de Ingeniería (UNI)
e-mail: rafaelg@ket.kh.se, phone (505) 270 1523
Apartado Postal 5595, Managua, Nicaragua

[2]Department of Chemical Engineering and Technology, Royal Institute of Technology (KTH)
jmc@ket.kth.se, phone (468) 790 6570
S-10044 Stockholm, Sweden

ABSTRACT

Liquid transport in capillary porous solids partially saturated with single liquids has been experimentally and theoretically studied. This work is focused on developing a method to determine the coefficient of liquid transport through solid materials containing liquid solvents.

Drying experiments of non-hygroscopic porous materials containing water and organic solvents were isothermally carried out in a jacketed wind tunnel, through which a humidity and temperature-controlled air stream flowed. The wetted porous material was placed in a cylindrical vessel exposed in the top to the air stream until the material became dried and the transient concentration profiles of the solvent along the cylindrical sample were determined. Different solvents and system temperatures were used with sand as solid.

Theoretical liquid content profiles have been obtained using a mathematical model that describes non-steady state isothermal drying of a solid containing a liquid. Hydraulic conductivity has been determined by comparing theoretical and experimental concentration profiles.

INTRODUCTION

Drying of products containing organic liquid is frequently seen in the process industry. Some examples include drying of pharmaceuticals, photographic films, magnetic storage media, varnish layers, coated laminates, and granulated synthetic materials.

In the study of drying of porous solids, internal mass and heat transfer are the most difficult steps to elucidate due to the complexity of the solid structure and the interaction between the different mechanisms involved in the process.

The existing theories take into consideration the solid structure and the manner in which the moisture is held within the solid to identify one or several of these mechanisms as dominating. The process is then described by conservation equations as functions of proper driving forces and transport parameters made accessible by either experiments or mathematical predictions. A review about the use of the available drying theories to describe drying of foodstuffs was presented by Fortes and Okos (1980). A summary of the advances in modeling the process was presented by Bories (1988). Further studies have recently been developed concerning mass transport and drying in solid porous media using different pore scale models: Prat (2002) summarized different contributions on pore-scale models. Perré and Turner (1999) simulated the drying process using a 3-D software, while Yiotis *et al* (2000) made their analysis with a 2-D network model.

The transport parameters involved in the theories are the hydraulic conductivity and the effective thermal conductivity. In an isothermal process, only the first is considered. The liquid transport coefficient, commonly called hydraulic conductivity has been a parameter widely studied by scientists devoted to drying of porous media and liquid infiltration, especially water containing solutes or water alone in soil research.

The methods for measurements of hydraulic conductivity are usually complex and the reliability is poor; thus different calculation methods based on other properties have been developed. Toei (1983) developed a method for drying porous solids, which requires measurements of capillary suction curves.

Reliable results have been obtained by combining experimental measurements and liquid transport

models. Perhaps the most used method have been the one developed by Van Genuchten (1980) beside others previously developed, i.e.: Mualem (1976). The Van Genuchten method consists in the estimation of fitting parameters from adjustment of theoretical models with experimental measurements. Studies of liquid transport had been done for water in both infiltration and drying processes. Büssing *et al* (1996) studied the isothermal transport of different liquids in packed beds obtaining the Van Genuchten parameters from experimental measurements of capillary pressures; however, they show the complexity generated by the phenomenon of hysteresis. Efforts for improving the reliability of hydraulic conductivity calculations from capillary pressure measurements have been done involving statistical methods as the maximum-likelihood estimation presented by Holenbeck and Jensen (1998).

This work is focussed on determining the hydraulic conductivity from drying experiments using different organic solvents as previous stage to the study of multicomponent liquid transport.

Comparing experimental and theoretical liquid content profiles, both hydraulic conductivity and capillary head pressure from the flux balance can be defined using the Van Genuchten parameters. Isothermal conditions simplifies the model because at constant temperature no differences in gas phase concentration exists within the solid bulk; in turn, gas diffusion does not contribute to the mass transfer.

THEORY

In an isothermal process, transport in liquid phase is the only mechanism that contributes to the mass transfer through a porous solid during surface drying. In the present study, particles of the bed are impermeable; therefore, mass transfer occurs only between particles, not within them. Under those conditions and taken into account that the porosity is uniform throughout the bed, the mass balance is described by the continuity equation:

$$\frac{\partial(\rho u)}{\partial t}+\frac{\partial(\rho v)}{\partial z}=0 \qquad (1)$$

where ρ is the liquid density, u the volumetric liquid content, v is the superficial velocity of the liquid, and z is the one dimension co-ordinate. In terms of volumetric flux, the expression becomes:

$$\frac{\partial u}{\partial t}=-\frac{\partial q}{\partial z} \qquad (2)$$

The volumetric flux of total liquid q is given as:

$$q=-\left\{D\frac{\partial u}{\partial z}-K\right\} \qquad (3)$$

The total mass balance can be arranged as:

$$\frac{\partial u}{\partial t}=\frac{\partial}{\partial z}\left\{D\frac{\partial u}{\partial z}-K\right\} \qquad (4)$$

The transport parameter D is sometimes called the liquid diffusivity. This parameter is not a properly diffusion coefficient but takes also into account the retention properties of the bed due to capillary forces. D is defined according to (Dullien 1992):

$$D=-K\frac{\partial h}{\partial u} \qquad (5)$$

where h is the capillary pressure head and K is the hydraulic conductivity given as:

$$K=\frac{\rho g \kappa k}{\mu} \qquad (6)$$

where ρ is the liquid density, g is the gravitational acceleration, κ is the relative permeability, k is the intrinsic permeability of the bed, and μ is the viscosity. Capillary pressure head and relative liquid permeability are defined by the functions developed by Van Genuchten (1980):

$$h=\frac{1}{\alpha}\left[\left(S_e^{1/\beta}-1\right)^{1/n}\right] \qquad (7)$$

$$S_e=\frac{u-u_{irr}}{u_{sat}-u_{irr}} \qquad (8)$$

$$\kappa=S_e^{1/2}\left[1-\left(1-S_e^{1/\beta}\right)^{\beta}\right]^2 \qquad (9)$$

where $\beta=1-1/n$. S_e is the effective saturation depending on u_{sat} (saturated liquid content) and u_{irr} (irreducible liquid content).

The irreducible liquid content is the minimum liquid content reached as the capillary pressure increases. The parameters n and α are obtained by fitting the shape of the curve to the experimental liquid content profiles.

To solve the total balance of equation (4), the following initially and boundary conditions are provided considering a uniform initial liquid content in bed. Initial condition:

$$u = u_0 \qquad 0 \le z \le 1 \qquad t = 0 \qquad (10)$$

Boundary condition at the bottom (isolated for both mass and heat transfer):

$$\frac{\partial u}{\partial z} = 0 \qquad z = 0 \qquad t > 0 \qquad (11)$$

Boundary condition at the top (convective evaporation):

$$-D\frac{\partial u}{\partial z} + K = -q(u) \qquad z = L \qquad t > 0 \qquad (12)$$

where *q(u)* is the volumetric liquid flux, which may be defined as a linear function of the liquid content since the bed is a non-hygroscopic material and does not requires an absorption isotherm.

$$q(u) = \frac{q_s - q(u_0)}{u_s - u_0}\left(u(t) - u_0\right) \qquad (13)$$

where u_0 is the minimum liquid content, in this case, $u_0 = 0$, $u(t)$ is the liquid content at the elapsed time, u_s and q_s are the liquid content and the volumetric flux at the saturation respectively. The volumetric flux is given by:

$$q_s = \frac{N_s}{\rho_\ell} \qquad (14)$$

where N_s is de evaporation rate obtained from a mass transfer correlation developed for the wind tunnel described in the experimental part, and ρ_ℓ is the density of liquid.

The model is a non-linear parabolic partial differential equation with no analytical solution. A numerical solution of finite differences was performed using the method of Crank Nicholson.

EXPERIMENTAL

Two types of experiments were carried out, isothermal drying of a non-hygroscopic porous solid to determine liquid content profiles, and evaporation of pure liquids to determine mass transfer coefficients in the equipment.

Drying Experiments

Set-up

To perform the drying experiments, the jacketed wind shown in figure 1 was used. Air taken from atmosphere by a blower was conducted through an adsorption column that reduced its humidity, then heated passing through a tube section with an electrical resistance. The hot and dried air stream flowed along the working section, which is the space within the jacketed portion of the tunnel.

Temperatures of the gas at the wet solid surface and the bulk were measured within the working section and recorded using thermocouples plugged to a computer. The gas temperature was controlled by an automatic control loop that regulated the energy supply to the electrical resistance placed in the tube section between the adsorption column and the wind tunnel.

Temperature-controlled water from a thermal bath circulated through the tunnel jacket side to guarantee isothermal conditions. The working temperature was set in both the air stream temperature control and the thermal bath.

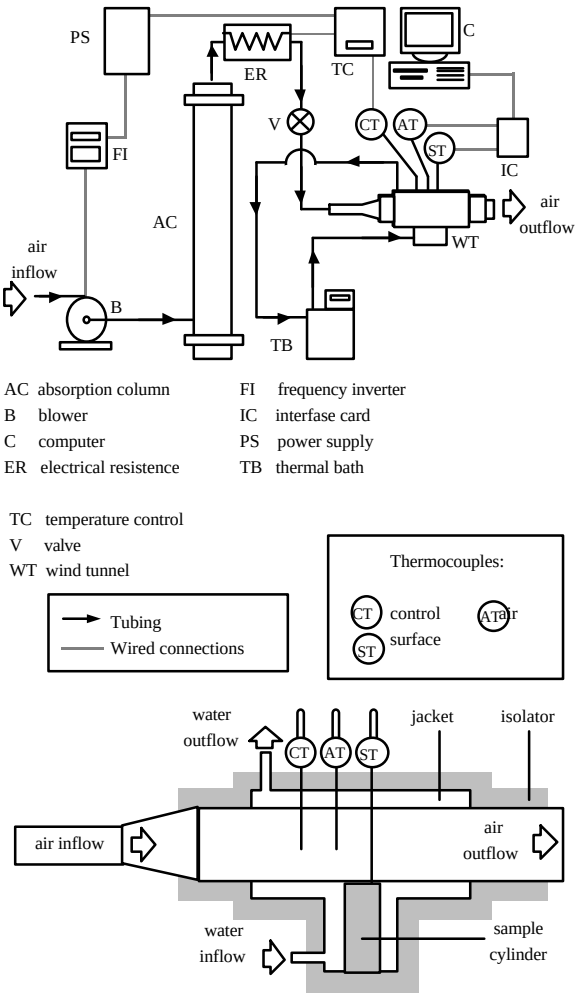

Fig. 1: Experimental set-up and detail of the wind tunnel section.

Procedure
The porous material was loaded in a cylindrical vessel divided in 10 rings of 1 cm high. Afterwards, the vessel containing the solid was filled with the solvent until the void volume became totally full.
After reaching stability at the set temperature and gas velocity, the vessel was placed in the jacketed portion of the wind tunnel perpendicular to the gas flow in such a way that the top open side was exposed to the air stream. Temperatures of the gas at the solid surface and the bulk started to be recorded once isothermal conditions were reached (Figure 2).

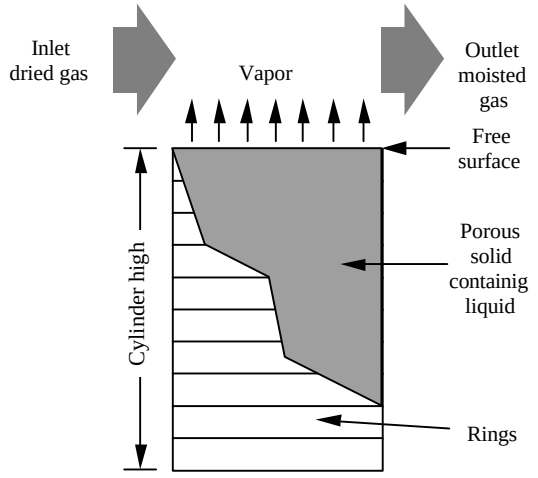

Figure 2: Sample cylinder and the evaporation at the free surface.

The physical models used as porous solid were glass beads (1 mm in diameter) and sand (0.125 – 0.250 mm in diameter). The behavior of single components was tested combining the conditions given in Table 1.

Table 1: Experimental conditions randomly combined used with single components, sand as solid, with v_g = 0.4050 m/s.

Component	Time t (h)	Temp. T (°C)
Water	0.5	40
Methanol	1.0	50
2 propanol	2.0	60

Experiment evaluation
After the exposure of the solid surface to the gas stream for a given time, the portion of solid from each ring was weighted, totally dried in an oven, and weighted again. The last mass measurement was the dried solid and the mass difference was the liquid mass contained in each ring at the end of the experiment. The liquid content is expressed as the ratio:

$$u = \frac{\rho_B}{\rho_\ell}\left(\frac{m_\ell}{m_B}\right) \qquad (15)$$

where u is the liquid content, ρ_B is the bulk density (solid apparent density), ρ_ℓ is the liquid density, m_ℓ is the liquid mass, and m_B is the mass o f dry solid.
Concentration profiles of the solvent were determined by plotting the liquid content of the solid against the cylinder high.

Porosity
The most suitable method to calculate the porosity ε of the bed was the method of effective porosity given by the relation of the void volume and the bulk volume. The void volume was filled with water until the bed was completely saturated, so that the volume of water V_w is equal to the previous void volume. The bulk volume V_B is the total volume of the containing vessel.

$$\varepsilon = \frac{V_w}{V_B} \qquad (16)$$

Mass Transfer Coefficients
Simulation runs require the rate of evaporation from the solid surface; therefore, a set of experiments was carried out in the wind tunnel with some adjustments to obtain mass transfer coefficients.

Set-up
A circular tray 0.54-cm in diameter and 1-cm high lying on analytical balance was placed instead of the cylindrical vessel inside the wind tunnel as shown in figure 3.

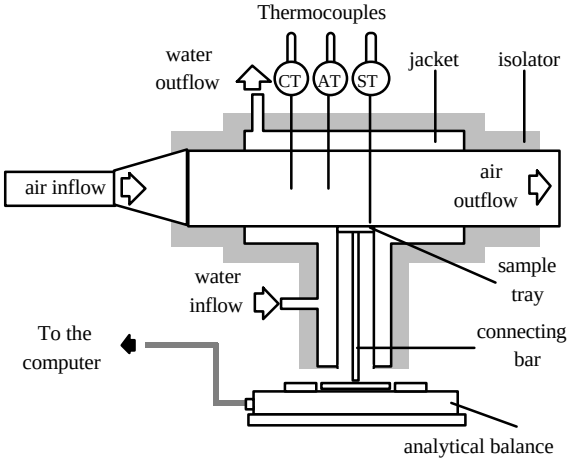

Figure 3: Wind tunnel with tray to calculate the evaporation rate at the surface.

Procedure
After reaching stability at the set temperature and gas velocity, the solvent was loaded in the tray using a syringe. Temperatures of the gas at the liquid surface and the bulk as well as the liquid mass change were measured and recorded in the computer. Two sets of experiments were run with the condition specified in Table 4.format used.

Table 4: Work conditions used in the experiments for the mass transfer coefficient correlation. Time for all runs was t = 1 h.

Water		
Exp. No.	Gas velocity v_g(m/s)	Temp. T(°C)
1	0.4050	40
2	0.7350	53
3	1.9950	60
2-propanol		
Exp. No.	Gas velocity v_g(m/s)	Temp. T(°C)
4	0.4050	32
5	0.5450	40
6	0.7350	50

Experiment evaluation
Mass change against time was plotted and the evaporation rate was computed as:

$$N = -\frac{1}{A}\frac{dm}{dt} \qquad (17)$$

where N is the evaporation rate m is the mass, t is the time, A is the tray area. The mass transfer coefficient h_D were calculated as:

$$h_D = \frac{N}{(C_s - C_B)M} \qquad (18)$$

where C_s and C_B are the concentrations of the vapor at the surface and the bulk respectively, and M is the molecular weight. Afterwards, the following set of dimensionless number were computed:

$$Sh = \frac{h_D d_s}{D_{vg}} \qquad \text{Sherwood number} \qquad (19)$$

$$\mathrm{Re} = \frac{\rho_g v_g d_s}{\mu_g} \qquad \text{Reynolds number} \qquad (20)$$

$$Sc = \frac{\mu_{vg}}{\rho_{vg} D_{vg}} \qquad \text{Schmidt number} \qquad (21)$$

where d_s is the surface diameter, and D_{vg} is the diffusivity of vapor in gas; ρ_g is the gas density, μ_g is de gas viscosity, and v_g is the gas velocity; μ_{vg} is the gas-vapor viscosity and ρ_{vg} is the gas-vapor density.

$$St = \frac{Sh}{\mathrm{Re}\,Sc} \qquad \text{Stanton number} \qquad (22)$$

$$J_D = StSc^{2/3} \qquad \text{Mass transfer factor} \qquad (23)$$

RESULTS AND DISCUSSION
Evaporation Rate at the Surface
Experiments at conditions listed in Table 4 were performed in the wind tunnel shown in Fig. 3. Mass changes with time from the experiments performed with water and 2-propanol are displayed in Figures 4 and 5 respectively. As expected, the evaporation rate is constant since a free liquid is evaporating at a constant temperature. Therefore, there is a linear variation of the mass as a function of time, and the derivative *dm/dt* is constant in each experiment.

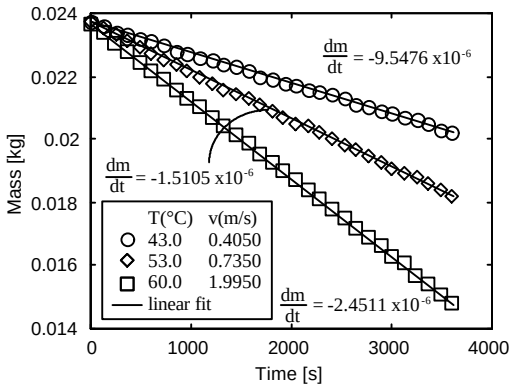

Figure 4: Change of mass with time of water at three temperatures and gas velocities.

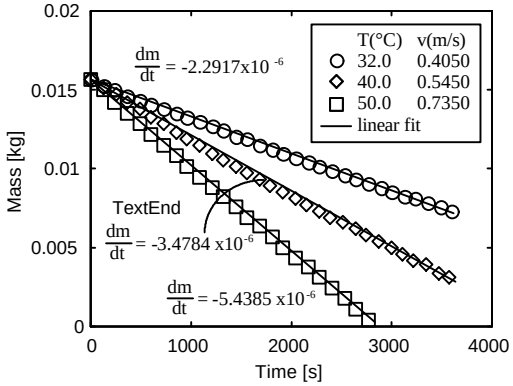

Figure 5: Change of mass with time of 2-propanol at three temperatures and gas velocities.

Evaporation rates were calculated introducing the slopes *dm/dt* from Figures 4 and 5 in equation (17), and mass transfer coefficients resulted from equation (18). Solving equations (19) throughout (23), the j-factor for mass transfer was obtained. It is as shown in Fig. 6 as a function of the Reynolds number.

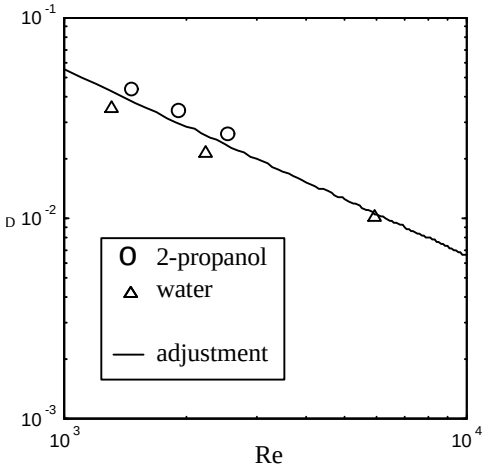

Figure 6: J-factor for mass transfer as a function of Reynolds number for evaporation from a free liquid surface in the wind tunnel.

Evaporation rates needed as boundary conditions for the main experiments were obtained by computing sequentially the Reynolds number from equation (20), the mass transfer factor from Fig. 6, and backward equations (17) throughout (23). Liquid volume fluxes resulted from equation (14).

Table 5: Summary of the evaporation rates and liquid volume fluxes of the tested solvents at different temperatures.

Solvent	Bulk temp. T_B (°C)	Surface temp. T_s (°C)	Evap. rate N_s (kg/m^2 s) x10^4	Liquid vol. flux q_s (m^3/m^2 s) x10^6
Water	40.0	27.5	4.34	0.44
	60.0	40.0	9.81	1.00
2-propanol	40.0	26.0	13.00	1.64
	60.0	37.3	29.00	3.78
Methanol	40.0	11.0	22.00	2.73
	50.0	16.5	15.00	1.93

As expected (see table 5), it is observed that the more volatile the liquids are the higher evaporation rate they exhibit. That is evident comparing the values of evaporation rate of each liquid at the same temperature (i.e.: 40°C), which are directly proportional to their corresponding vapor pressures at the surface.

Porosity

Porosity of the solid was calculated with the method of equation (13). The resulting value was $\varepsilon = 0.43$. The vessel containing the solid was filled in such a way that the ratio liquid volume / bulk volume (initial liquid content, u_0) were the same. In order to avoid loses of liquid during the placement of the cylinder into the tunnel the initial liquid content was slightly smaller than the porosity. Thus, $u_0 = 0.42$.

Liquid Content Profiles

Experiments of liquid transport were performed in the wind tunnel shown in Fig.3. The experiments were divided in 3 different sets as follow:

- Water in sand at 60°C for 0.5, 1.0 and 2.0 h periods (3 experiments).
- 2-propanol in sand at 60°C and 40°C for 0.5, 1.0 and 2.0 h periods (6 experiments).
- Methanol in sand at 50°C for 0.5 and 1.0 h; and at 40°C for 1.0 h (3 experiments).

The liquid content profiles obtained in the drying experiments are represented in Figures 7 throughout 18. Measured values of experimental liquid distribution are represented by circles and the profile from simulation is represented by the continue curve. The10-cm high bed is divided in 10 segments. Every liquid content measured in each 1-cm segment was considered a mean value along the segment.

Adjustment of theoretical curves was made fitting de Van Genuchten parameters (n, α) in such a way that satisfied the liquid distribution at the different elapsed times. The adjusting program solved the model fed with the experimental values in an iterative calculation until the theoretical curve matched with the experimental profile. The slight differences exhibited by these parameters when the same system was dried during different times at the same temperature, depend rather on experimental uncertainties, mean values of the fit parameters are displayed in Table 6. The same mean values were used in the simulations.

Table 6: Irreducible liquid content, Van Genuchten parameters and bed permeability fit for the experiment carried out.

Liquid	Temp. T (°C)	u_{irr} x 10^2	α x 10^1
Water	60.0	3.9477	98.246
2-propanol	60.0	1.9446	8.7745
	40.0	1.4842	9.4150
Methanol	50.0	1.3961	7.4842
	40.0	2.2281	8.8800

Liquid	Temp. T (°C)	n x 10^{-2}	k x 10^{13}
Water	60.0	0.5654	1.37
2-propanol	60.0	0.9765	2.50
	40.0	1.5610	2.50
Methanol	50.0	2.0846	2.50
	40.0	2.6011	2.50

As shown in Figures 7 to 18, the mean values satisfied fairly the experimental profiles at the different elapsed times.

The bed permeability (k) is of order 10^{-13} in all cases although in the water experiments it was lower probably because the bed was more compact in these experiments.

The transient distribution for water displayed in Figures 7-9 revealed that when the time increases the liquid content gradients at the surface are reduced.

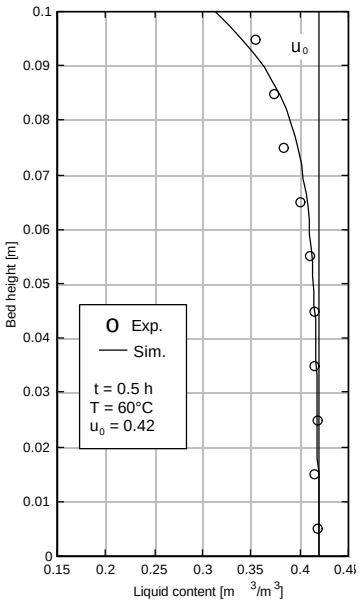

Figure 7: Liquid content profile of water at 60°C and 0.5 h.

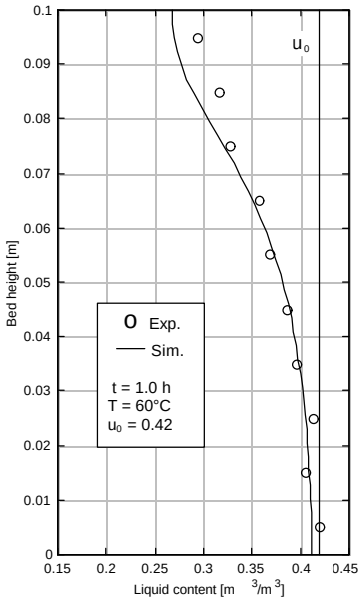

Figure 8: Liquid content profile of water at 60°C and 1.0 h.

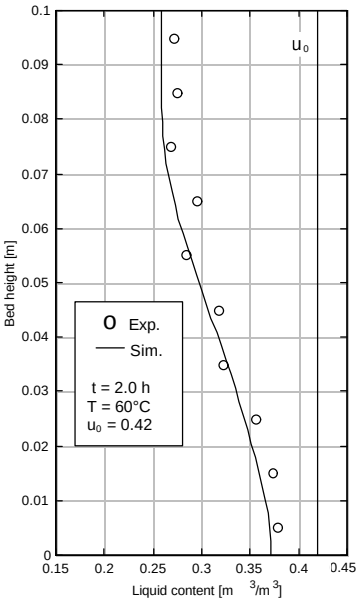

Figure 9: Liquid content profile of water at 60°C and 2.0 h.

A plausible explanation is that the drying conditions at the surface changes with time, causing a decrease of the drying rate. In the new conditions, to provide liquid by capillarity to the surface demands smaller liquid content gradients.

A comparison with the transient liquid distributions for 2-propanol displayed in Figures 10-12, revealed that beside an increase of solvent removal, the gradients of liquid content at the surface are larger for 2-propanol than for water. The drying rate of 2-

propanol is higher than the drying rate of water because of the higher relative volatility of 2-propanol compared to water. In addition, the liquid transport inside the solid is slower for 2-propanol than for water. Both factors contribute to larger liquid content gradients and lower liquid content at the surface for 2-propanol. Of course, as the time increases and the conditions at the surface are less demanding the gradients at the surface diminishes even for 2-propanol.

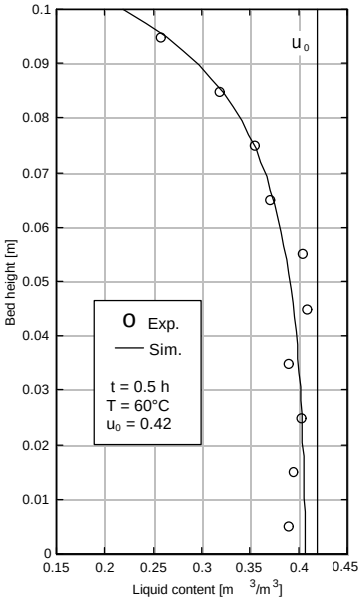

Figure 10: Liquid content profile of 2-propanol at 60°C and 0.5 h.

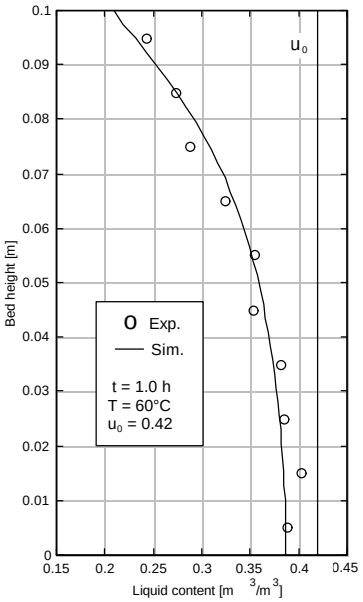

Figure 11: Liquid content profile of 2-propanol at 60°C and 1.0 h.

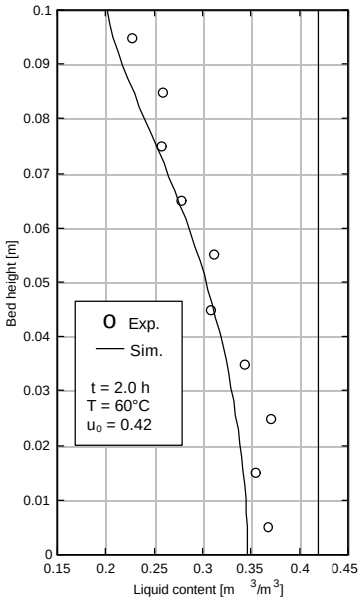

Figure 12: Liquid content profile of 2-propanol at 60°C and 2.0 h.

Figures 13-15 displays the liquid distribution of 2-propanol at 40°C. The shapes are similar to those at 60°C, but since the evaporation rate is lower at a lower temperature the remaining liquid content corresponding to the same times is higher. As the external conditions are less demanding, the gradients of liquid content at the surface are smaller. It is particularly noticeable in the 2 hours experiment when the evaporation at the surface has been significantly reduced.

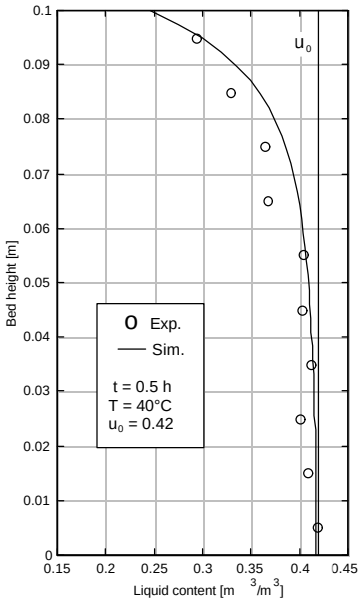

Figure 13: Liquid content profile of 2-propanol at 40°C and 0.5 h.

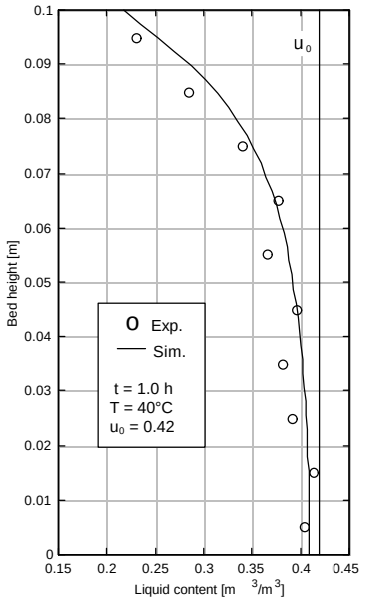

Figure 14: Liquid content profile of 2-propanol at 40°C and 1.0 h.

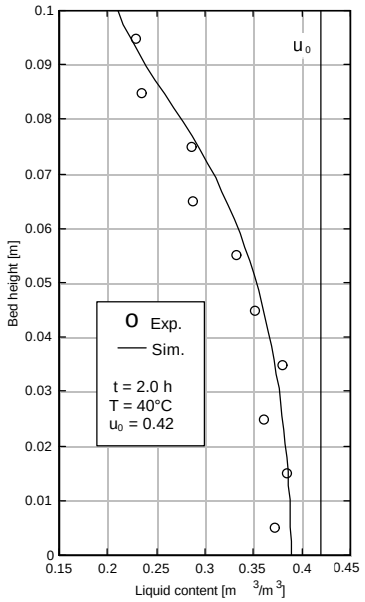

Figure 15: Liquid content profile of 2-propanol at 40°C and 2.0 h.

The last set of plots of Figures 16-18 corresponds to methanol. The liquid content at the surface for methanol is lower than the one of 2-propanol and water in that order, which is understandable since the higher the volatility the higher the evaporation rate. The profile of methanol at lower temperature (Figure 18) shows the same behavior as that of 2-propanol.

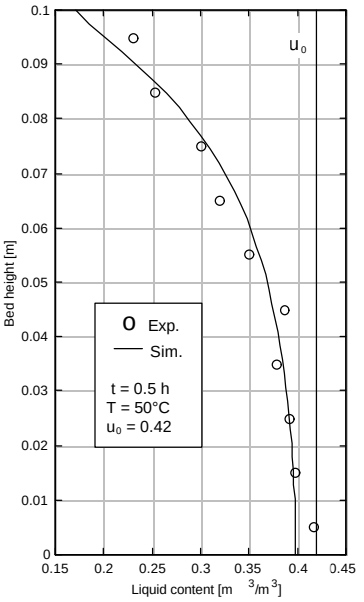

Figure 16: Liquid content profile of methanol at 50°C and 0.5 h.

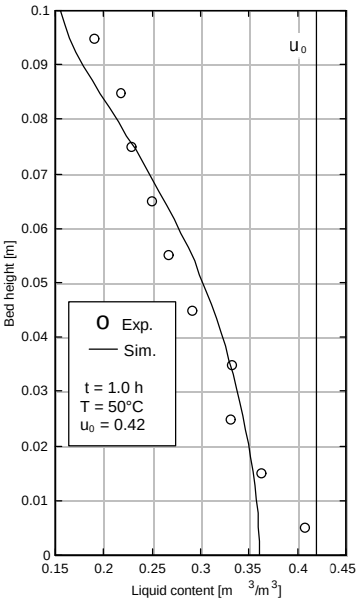

Figure 17: Liquid content profile of methanol at 50°C and 1.0 h.

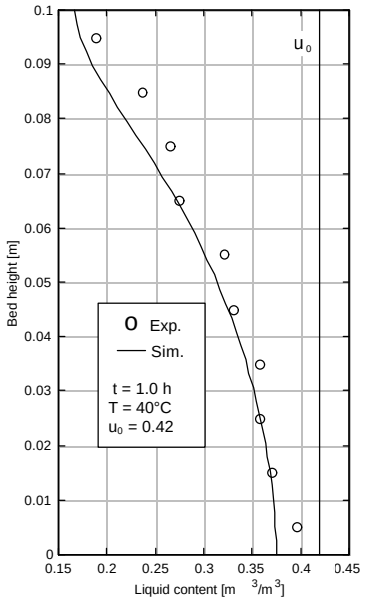

Figure 18: Liquid content profile of methanol 40°C and 1.0 h.

Influence of Temperature

Temperature influenced on liquid migration through the bed in both ways: the rate of evaporation and the liquid transport itself. Temperature is directly associated with the vapor pressure at the surface, thus influences directly on the drying rate since the difference of concentration between the surface and the gas bulk increases with the temperature.

The influence of temperature on liquid transport is related to the dependence of the hydraulic conductivity on density and viscosity as well as the influence of surface tension on the capillarity and thereby on the liquid diffusivity. These physical properties are functions of temperature. The influence of density and viscosity stands in equation (4). Since density is divided by viscosity and both of them increase with temperature, the total contribution of the ratio is small, so that the temperature has a limited influence on the hydraulic conductivity. Figures 19 to 20 show the hydraulic conductivity as function of saturation corresponding to the experiment carried out with 2-propanol, methanol and water respectively.

In order to elucidate the influence of the temperature on the hydraulic conductivity of water calculations at two additional temperatures (keeping the parameters determined at 60°C) are shown in Figure 21.

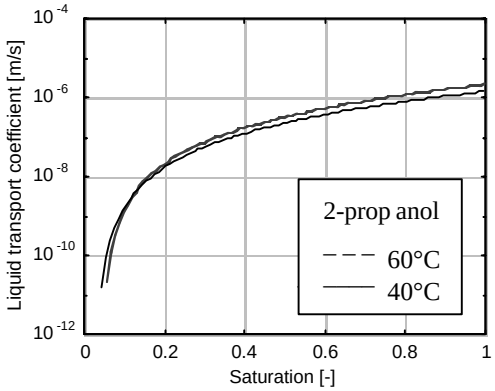

Figure 19: Hydraulic conductivity of 2-propanol at 40°C and 60°C.

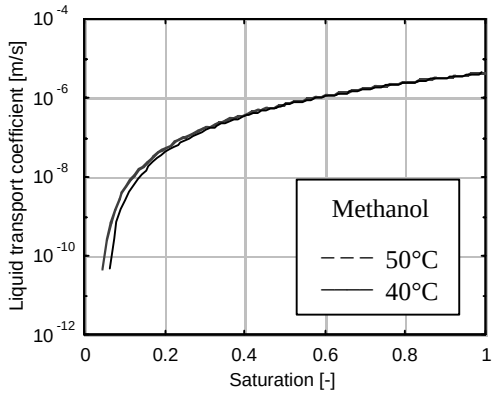

Figure 20: Hydraulic conductivity of methanol at 40°C and 50°C.

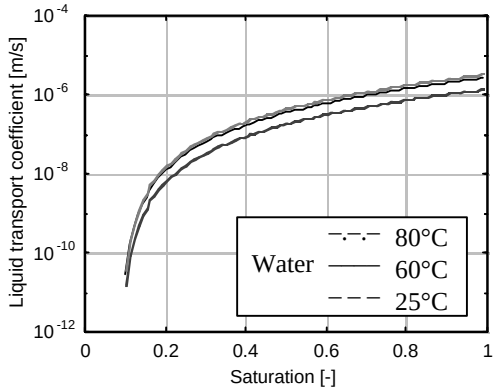

Figure 21: Hydraulic conductivity of water at 25°C, 60°C and 80°C.

The effects of temperature on the other factor that influence liquid transport within the solid, the liquid diffusivity, may be observed in Figures 22, 23, and 24 for 2-propanol, methanol and water respectively. As in the case of the hydraulic conductivity the influence of temperature is limited. Although temperature has less influence than liquid content on both hydraulic

conductivity and liquid diffusivity, the effects of temperature on liquid transport cannot be neglected in non-isothermal processes. That must be considered particularly when large temperature gradients are present as in the case of contact drying.

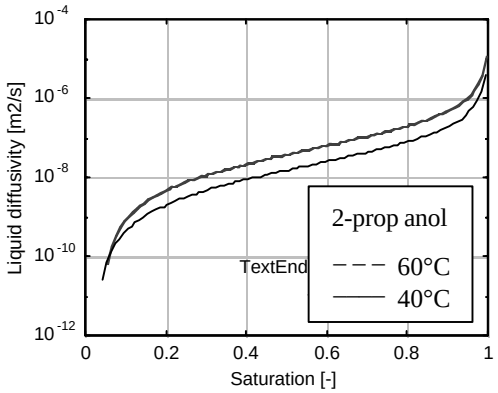

Figure 22: Liquid diffusivity of 2-propanol at 40°C and 60°C.

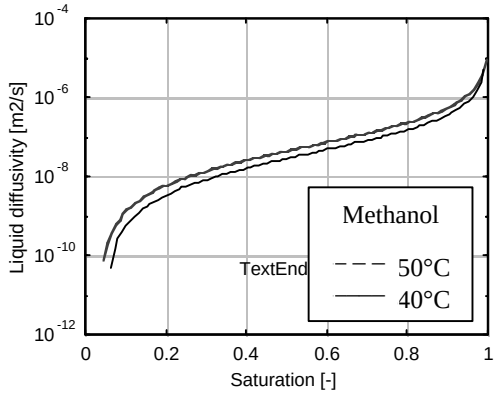

Figure 23: Liquid diffusivity of methanol at 40°C and 50°C.

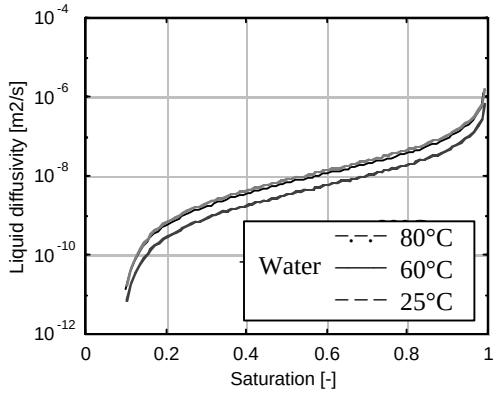

Figure 24: Liquid diffusivity of water with parameters tested at 60°C.

CONCLUSIONS

Isothermal liquid transport during drying of a porous solid initially sutured with a liquid was experimentally and theoretically studied. Experiments were performed with water, 2-propanol and methanol as single liquids and sand as porous media.

Transport coefficients described by Van Genuchten parametric model were determined by comparing experimental liquid content profiles with simulated profiles.

Drying experiments carried out at different temperatures show a limited influence of temperature on the transport coefficients; in turn the foremost notorious increase of drying velocity with temperature is consequence of it effect on evaporation rate at the surface.

On the other hand, the transport coefficients are strong dependent on the liquid content or degree of saturation.

Isothermal drying experiments are a suitable and simple method to determine the transport parameters, which account for the movement of liquid within the solid, the hydraulic conductivity and liquid diffusivity.

NOTATION

Latin letters

A	area	(m^2)
C	concentration	(kmol m^{-3})
d	diameter	(m)
D	diffusivity	(m^2 s^{-1})
g	gravitational constant	(m s^{-2})
h	pressure head	(m)
h_D	mass transfer coefficient	(m s^{-1})
J_D	mass transfer factor	-
k	intrinsic permeability	-
K	hydraulic conductivity	(m s^{-1})
L	bed high	(m)
m	mass	(kg)
n	parameter	-
N	mass flux (evaporation/drying rate)	(kg m^{-2} s^{-1})
P	total pressure	(N m^{-2})
q	volume flux	(m^3 m^{-2} s^{-1})
Re	Reynolds number	-
S	saturation u/ε	(m^3 liq.m^{-3} pore)
Sc	Schmidt number	-
Sh	Sherwood number	-
St	Stanton number	-
t	time	(s)
T	temperature	(K)
u	liquid content	(m^3 liq.m^{-3} tot)
v	velocity	(m s^{-1})
V	volume	(m^{-3})
z	length coordinate	(m)

Greek letters

α	parameter	-
β	parameter	-
ε	solid porosity	-
ρ	density	(kg m^{-3})
κ	relative permeability	-

Subscripts

B	denotes bulk	*s*	surface
e	effective	*sat*	saturation
g	gas	*0*	initial
irr	irreducible	*v*	vapour
ℓ	liquid phase	*w*	water

REFERENCES

Bories S., (1988), "Recent Advances in Modelisation of Coupled Heat and Mass Transfer in Capillary-Porous Bodies. Sixth International Drying Symposium," IDS'88, Versailles, KL.47-61.

Büssing W., Bart H.J., Germerdonk R., (1996), "Isothermal Liquid Transport in Porous Media: Capillary Hysteresys Effect," Int. J. Heat Mass Transfer, vol. 39, pp 1925-1934.

Dullien F. A. L., (1992), "Porous Media: Fluid Transport and Pore Structure," 2nd ed., Academic Press, STAD.

Fortes M. and Okos M. R., (1980), "Drying Theories: Their Bases and Limitations as Applied to Foods and Grains," pp 119-154. In: Advances in Drying, vol. 1. Ed. A.S. Mujumdar.

Hollenbeck K.J., Jensen K.H., (1998), "Maximum-likelihood Estimation of Unsaturated Parameters," J. of Hydrology 210, pp 192-205.

Mualem Y., (1976), "A New Model for Predicting the Hydraulic Conductivity of Unsaturated Porous Media," Water Resour. Res. 12 (3), pp 513-522.

Perré P. and Turner I., (1999), "A 3-D Version of TransPore: A Comprehensive Heat and Mass Transfer Computational Model for Simulating the Drying of Porous Media," Int. J. of Heat and Mass Trans, pp 4501-4521.

Prat M., (2002), "Recent Advances in Pore-scale Models for Drying of Porous Media," Chem. Eng. J, pp 153-164.

Toei R., (1983), "Drying Mechanism of Capillary Porous Bodies," pp 269-297. In: Advances In Drying, Vol. 2. Ed. A.S. Mujumdar.

Van Genuchten T., (1980), "A Closed Form Equation for Predicting the Hydraulic Conductivity of Unsaturated Soils," Soil Sci. Soc. Am., 44.

Yiotis A., Stubos A., Boudouvis A., Yortsos Y.,(2000), "A 2-D Pore-network Model of the Drying of Single-component Liquids in Porous Media," Adv. in Water Resources., pp 439-460.